Highly active Cu-MFI catalyst for conversion of furfuryl alcohol to pentanediols

Dengfeng Dai [1], Dandan Liu [1, 2, *] and Yunqi Liu [1]

[1] State Key Laboratory of Heavy Oil Processing, China University of Petroleum (East China), Qingdao 266580 (China)
[2] College of New Energy, China University of Petroleum (East China), Qingdao 266580 (China).

Abstract. It is of great significance to use biomass-based furfuryl alcohol to produce oxygenated chemicals to replace petroleum-based chemicals. In this paper, a series of bifunctional Cu-MFI catalysts were developed, and the properties of biomass-based furfuryl alcohol to pentanediol, including 1,5-pentanediol and 1,2 pentanediol, were investigated. These catalysts were synthesized by ammonia evaporation method by loading copper nanoparticles on MFI molecular sieve systems with different silicon aluminum ratios. Among them, Cu-MFI (60)-AE catalyst containing abundantly Brønsted acid protons shows excellent performance, achieving 99.7% furfuryl alcohol conversion and 91% pentanediol selectivity under mild reaction conditions. The high catalytic activity can be attributed to the highly dispersed Cu species and Brønsted acid protons. Brønsted acid protons play a decisive role in the highly selective formation of 1,5-PDO. This paper can develop an economical and feasible path for converting furfuryl alcohol into high value-added fine chemicals.

1. Introduction

The preparation of fine chemicals from biomass as a substitute for petrochemical resources has attracted increasing attention[1]. Furfuryl alcohol (FFA), as a semi hydrogenation product of furfural, is an important biomass resource and has been widely used in industry[2,3]. FFA is an important renewable chemical, which can be transformed into a variety of high value-added chemicals through chemical paths[4,5]. The ring opening products of FFA are important diols, such as 1,5-pentanediol (1,5-PDO) and 1,2-pentanediol (1,2-PDO). Because C5 petroleum based raw materials are difficult to obtain[6,7], the route to obtain pentanediol from FFA is a sustainable reaction, which has significant economic prospects.

Copper based catalysts have been used in various oxygenated chemical transformations[8,9]. Chen's team explored the catalytic performance of Cu-$LaCoO_3$, Cu-LDO and Cu/Al_2O_3 bifunctional catalysts[10-12]. Cu/Al_2O_3 catalyst achieved 85.8% FFA conversion and 70.3% PDO selectivity under 8.0 MPa H_2. Jones research group realized 62% PDO yield by using reduced Cu-Co-Al mixed metal oxides[10-12]. These reactions are generally carried out under intermittent conditions of high hydrogen pressure, and the selectivity of 1,5-PDO is far from satisfactory.

Herein, we developed a bifunctional Cu-MFI catalyst by loading uniform copper nanoparticles on MFI zeolite by ammonia evaporation, which achieved 99.7% FFA conversion and 91% PDO selectivity under continuous conditions. The excellent activity achieved can be attributed to the cooperation between highly dispersed Cu species and Brønsted acid protons.

2. Experimental

2.1 Synthesis of Cu-MFI (60)-AE, Cu-MFI (130)-AE and Cu-MFI (Si)-AE

Three catalysts adopted HZSM-5 (SiO_2/Al_2O_3= 60, 130) and silicalite-1 as support and synthesized by ammonia evaporation methods with 3.0 wt.% Cu content, respectively. denoted as Cu-MFI (60)-AE, Cu-MFI (130)-AE and Cu-MFI(Si)-AE, respectively. The three samples were reduced under a flow of H_2 at 300°C for 2 h, and named as Cu-MFI (60)-AER, Cu-MFI (130)-AER, and Cu-MFI(Si)-AER, respectively.

2.2 Catalyst characterization

The catalyst characterization was carried out on X'pert Pro MPD X-ray diffractometer, ASAP 2020 microporous physical adsorption analyzer, JEOL JEM-2100F microscope, escalabmk X-ray photoelectron spectrometer, vertex 70 Fourier transform infrared spectrometer, AutoChem 2950 HP instrument, and IRIS Intrepid II XSP instrument.

2.3 Catalytic testing and product analysis

The products were analyzed by Agilent 7820a GC with HP-5 column; the conversion of FFA and pentanediol selectivity was calculated by the following formula:

$$\text{Conversion} = \frac{[\text{FFA}]\text{f} - [\text{FFA}]\text{p}}{[\text{FFA}]\text{f}} \times 100\% \quad (1)$$

* Corresponding author: liudandan@upc.edu.cn

$$\text{Selectivity} = \frac{[\text{PDO}]p}{[\text{FFA}]f - [\text{FFA}]p} \times 100\% \quad (2)$$

[FFA]f is the FFA content in the feedstock (%) and [FFA]p is the FFA content in the products (%); [PDO]p is the 1,2-PDO and 1,5-PDO content in the products (%).

3. Results and discussion

3.1 Characterization of copper-based catalysts

Table 1. Basic physical properties of catalysts

Catalyst	[a]Cu/wt%	[a]SiO_2/Al_2O_3	[b]$S/m^2 \cdot g^{-1}$	[c]$V/cm^3 \cdot g^{-1}$	[d]D_{Cu}/nm
Cu-MFI (60)-AE	2.6	57	323	0.20	2.5
Cu-MFI (130)-AE	2.7	129	306	0.18	--
Cu-MFI(Si)-AE	2.9	--	320	0.18	--

(a) Obtained by ICP-OES. (b) Total surface area. (c) Total pore volume. (d) Average particle size of Cu species from HRTEM

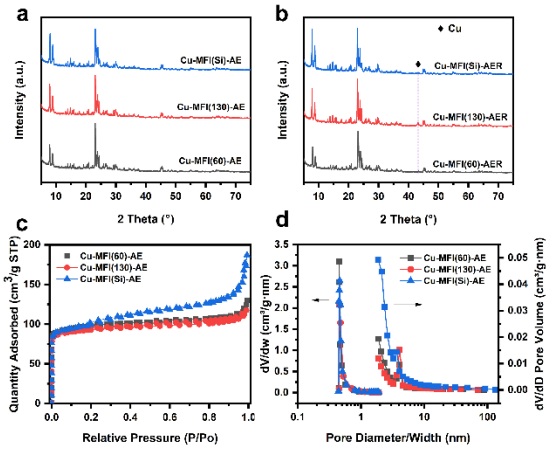

Figure 1. X-ray diffraction patterns of the (a) calcined catalysts, (b) reduced catalysts. (c) Nitrogen adsorption-desorption for calcined catalysts, (d) corresponding pore size distribution.

The XRD of calcined catalysts were shown in Figure 1a. All samples show a typical structure of MFI. No diffraction peak of CuO was found at 35.5o and 38.7o, indicating that CuO was evenly distributed on the surface of zeolite. After reduction, a weak diffraction peak attributed to Cu (111) appears at 43.3o, indicating that the species of Cu were evenly distributed. Nitrogen adsorption-desorption curves (Figure 1c) show that adsorbed rapidly at low pressure, and no hysteresis loop was found at 0.4-1.0P/Po, indicating that all three catalysts were typical microporous structures[14]. It was also confirmed by the corresponding pore size distribution (Figure 1d). The corresponding porous property data were also summarized in Table 1. In addition, ICP-OES showed that copper loading was close to theoretical value.

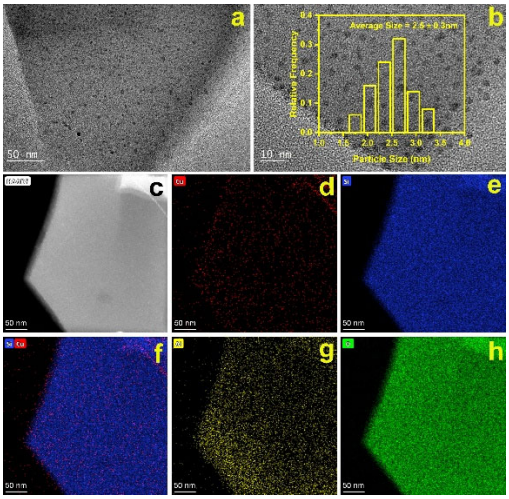

Figure 2. (a, b) HRTEM images for Cu-MFI (60)-AER, with corresponding size distributions of Cu species. (c-h) HAADF-STEM images, and corresponding EDS-mapping of Cu, Si, Si + Cu, and Al, O element.

HRTEM and HADDF-STEM were used to investigate the metal distribution on the catalyst surface, as shown in Figure 2. HRTEM images (Figure 2a, 2b) show that the distribution of copper particles is uniform, and no obvious particle agglomeration is found, which is consistent with the results of XRD. The average particle size of copper particles is 2.5nm. HADDF-STEM images and the corresponding EDS-mapping images show that copper and other elements are interlaced, indicating that Cu is evenly distributed on the surface of zeolites. This can improve the utilization of metal and promote the reaction.

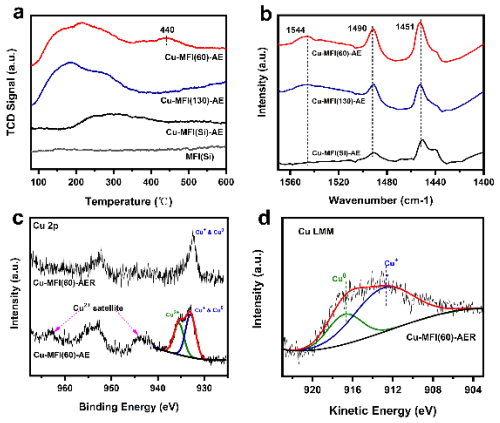

Figure 3. (a) NH3-TPD profiles of different catalysts and MFI(Si) support. (b) Pyridine infrared (Py-IR) spectrum profiles of catalysts. (c) Cu 2p XPS spectrum of Cu-MFI (60)-AE and Cu-MFI (60)-AER. (d) Cu LMM XAES spectrum of Cu-MFI (60)-AER.

To reveal the effect of surface acidity on ring opening of FFA, NH_3-TPD and Py-IR were used to investigate the surface acidity of the catalyst. The results are shown in Figure 3a and 3b. Cu-MFI (60)-AE shows a continuous

desorption peak of NH_3 at 100-500 ℃. The NH_3 desorption peak at 440 ℃ is attributed to the strong interaction between NH_3 and Brønsted acid protons. Cu-MFI (130)-AE shows a continuous desorption peak at 100-380 ℃, and its strong acid content is lower than that of Cu-MFI (60)-AE, which is determined by the number of framework Si $(OH)^+$ Al unit[15]. However, Cu-MFI(Si)-AE shows a small desorption peak, and the corresponding MFI(Si) has no NH_3 desorption peak, indicating that the NH_3 desorption peak of Cu-MFI(Si)-AE is mainly caused by the interaction between NH_3 and copper species.

The three samples showed obvious characteristic bands at 1451 cm^{-1} and 1490 cm^{-1}, which were attributed to Lewis acid and Brønsted + Lewis acid, respectively. The difference was that Cu-MFI (60)-AE and Cu-MFI (130)-AE present a characteristic bands of 1544 cm^{-1}, corresponding to Brønsted acid[16], indicating that there were Brønsted acid protons in the catalysts. This was determined by the density of framework Si $(OH)^+$ Al unit of the support. and there is no Brønsted acid protons in Cu-MFI(Si)-AE.

The surface metal valence plays an important role in the ring opening of FFA. It was reported that unsaturated Cu^+ acts as anchoring sites for -CH_2OH, while Cu mainly plays the role of hydrogen activation. XPS and Cu LMM XAES were used to analyze the surface chemical state, and the results are shown in Figures 3c and 3d. After calcination, an obvious satellite peak appeared at binding energies of 943 eV for Cu-MFI (60)-AE catalyst, indicating the presence of Cu^{2+} species in the sample[17]. In addition, two overlapping peaks are found at 935.5 eV and 933.0 eV, corresponding to Cu^{2+} and Cu^0 and/or Cu^+ species[8], respectively. These indicate that part Cu^{2+} was reduced to Cu^+ and/or Cu during the roasting process, which may be exerted by the decomposition gas of NH_4^+ in the zeolite during the roasting process. The decomposition gas caused the reduction of copper, this is similar to that reported. After the reduction, the satellite peak disappeared, indicating that Cu^{2+} species were reduced to Cu^+ and/or Cu. The species composition was further analyzed using Cu LMM XAES, and an asymmetric peak was detected at 915.9 eV and 913.0 eV, which belong to Cu^0 species and Cu^+ species, respectively. This illustrated the coexistence of Cu^+ and Cu^0 species on the surface.

3.2 Catalysts performance for the FFA ring-opening to pentanediols

Scheme 1. Reaction pathway of FFA for different catalysts

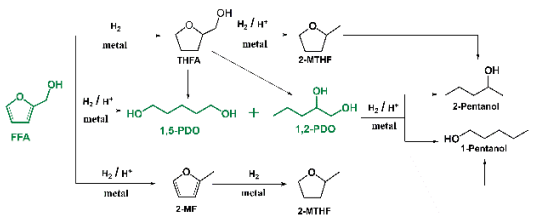

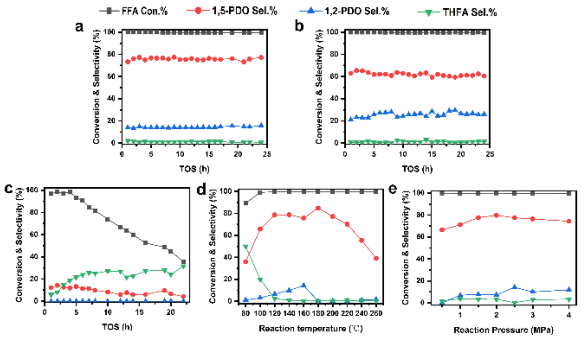

Figure 4. Catalyst performance test of (a) Cu-MFI (60)-AE, (b) Cu-MFI (130)-AE, (c) Cu-MFI(Si)-AE, 160 ℃, 2.5 MPa H2. (d) catalyst performance test at different reaction temperature. (e) catalyst performance test at different H2 pressure.

The highly selective ring opening of FFA is an ideal path to obtain PDO (Scheme 2). The activity of Cu-MFI (60)-AE, Cu-MFI (130)-AE, and Cu-MFI(Si)-AE was tested at 160 ℃ and 2.5 MPa H_2, respectively. The results are shown in Figure 4. Cu-MFI (60)-AE catalyst exhibits excellent selectivity for PDO, which achieved a nearly 100% FFA conversion with a 91% selectivity for PDO, including 76% selectivity of 1,5-PDO and 15% selectivity of 1,2-PDO. Cu-MFI (130)-AE catalyst also achieved 87.7% PDO selectivity at nearly 100% conversion. The selectivity of 1,5-PDO reduces from 76% to 62%, while the selectivity of 1,2-PDO increases from 15% to 26% with the increase of SiO_2/Al_2O_3 ratios. This is closely related to the density of Brønsted acid protons, demonstrating that Si$(OH)^+$Al could promote the formation of 1,5-PDO. Cu-MFI(Si)-AE catalyst showed low activity and selectivity. The conversion of FFA gradually decreased from 96% to 36%, while the highest selectivity of 1,5-PDO was only 14%, and no 1,2-PDO was observed. The difference in activity and selectivity mainly comes from the difference in Brønsted acid protons in the catalyst. This means that Brønsted acid protons are the key factor to promote the ring opening of FFA

In addition, the effects of reaction temperatures and pressures on the ring opening of FFA were also investigated. With the increase of reaction temperature, the selectivity of 1,5-PDO increased first and then decreased. The selectivity of 1,5-PDO reached the maximum value of 84.9% at 180 ℃, surpassing the previously reported non-noble metal catalysts. The selectivity of 1,2-PDO was reduced to <2% after the temperature exceeded 180 ℃, this may be caused by further dehydration of 1,2-PDO under high temperatures. Hydrogen pressure has little effect on the selectivity of FFA ring opening. nearly 100% conversion and 66% selectivity of PDO can still be achieved even at a low pressure of 0.5 MPa, demonstrating that acidity is the main factor determining the ring opening rather than hydrogen pressure.

4. Conclusions

In conclusion, a bifunctional Cu-MFI catalyst with high activity and selectivity was prepared for the ring opening

of FFA to pentanediol. The catalyst with abundantly Brønsted acid protons and highly dispersed copper species exhibits excellent performance. Among them, Brønsted acid protons are stem from molecular sieve support, and highly dispersed copper species derived from the ammonia evaporation preparation process. The yield of pentanediol is more than 91% in 24 h TOS. The excellent activity is superior to the previously reported non-noble metals, and the activity selectivity is comparable to that of noble metal catalysts. This study provides a new idea for the low-cost synthesis of pentanediol from biomass-based materials.

Acknowledgements

This work has been financially supported by the National Natural Science Foundation of China (22005342).

References

1. T. Zhang, W. Li, H. Xiao, Y. Jin, S. Wu, Bioresour. Technol. 2022, 354, 127126.
2. Z. Chen, X. Bai, A. Lusi, W. A. Jacoby, C. Wan, Bioresour. Technol. 2019, 289, 121708.
3. S. Liu, N. Govindarajan, K. Chan, Acs Catal. 2022, 12902-12910.
4. X. Li, P. Jia, T. Wang, Acs Catal. 2016, 6, 7621-7640.
5. R. Mariscal, P. M. Ojeda, I. Sádaba, M. López Granados, Energy Environ. Sci. 2016, 9, 1144-1189.
6. G. Hayes, M. Laurel, D. MacKinnon, T. Zhao, H. A. Houck, C. R. Becer, Chem. Rev. 2022.
7. D. Sun, S. Sato, W. Ueda, A. Primo, H. Garcia, A. Corma, Green chemistry. 2016, 18, 2579-2597.
8. Z. Zhang, Z. L. Wang, K. An, J.. Song, Y. Bando, Y. Yamauchi, Y. Liu, Small. 2021, 17, 2008052.
9. D. Dai, C. Feng, M. Wang, Q. Du, D. Liu, Y. Pan, Y. Liu, Catal. Sci. Technol. 2022, 12, 5879-5890.
10. H. Liu, Z. Huang, F. Zhao, F. Cui, X. Li, C. Xia, J. Chen, Catal. Sci. Technol. 2016, 6, 668-671.
11. Fangfang Gao, H, J. Chen, Z. Huang, C. Xia, Chinese Journal of Catalysis. 2018, 39, 1711-1723.
12. H. Liu, Z. Huang, H. Kang, C. Xia, J. Chen, Chinese Journal of Catalysis. 2016, 37, 700-710.
13. T. P. Sulmonetti, B. Hu, S. Lee, C. W. Jones, Acs Sustain. Chem. Eng. 2017, 5, 8959-8969.
14. M. Thommes, K. Kaneko, A. V. Neimark, J. P. Olivier, F. Rodriguez-Reinoso, J. Rouquerol, K. S. W. Sing, Pure Appl. Chem. 2015, 87, 1051-1069.
15. P. Arudra, T. I. Bhuiyan, A. M. Aitani, S. S. Al-Khattaf, H. Hattori, Acs Catal. 2014, 4, 4205-4214.
16. F. Yaripour, Z. Shariatinia, S. A. Irandoukht, Microporous Mesoporous Mat. 2015, 203, 41-53.
17. R. Ye, L. Lin, C. Chen, J. Yang, F. Li, X. Zhang, D. Li, Y. Qin, Z. Zhou, Y. Yao, Acs Catal. 2018, 8, 3382-3394.